Crop Classification Using Time-Series Landsat Data: A Comparison of Attention-Based LSTM, GRU, and TCN Models

Yuta Tsuchiya[1], Rei Sonobe[1]

[1] Graduate School of Science and Technology, Shizuoka University, Shizuoka, Japan

Keywords: Crop classification; Precision agriculture; Temporal modeling; Satellite remote sensing

Abstract

This study aimed to develop a highly accurate crop classification framework using multi-temporal Landsat 9 imagery and advanced deep learning architectures for the Tokachi Plain, a major agricultural region in Japan. Six time-series scenes, acquired between May 2 and September 16, 2024, were used to classify six crop categories: beans, beetroot, grassland, maize, potato, and winter wheat. Three temporal models with attention mechanisms were evaluated: long short-term memory (LSTM), bidirectional gated recurrent unit (Bi-GRU), and temporal convolutional network (TCN). Of the models tested, the TCN + Attention architecture achieved the highest overall accuracy (81.3%), significantly outperforming LSTM and Bi-GRU ($p < 0.001$). The Near-Infrared (NIR) band (Band 5) consistently exhibited the highest importance, highlighting its sensitivity to vegetation structure and chlorophyll content. Despite relying on only six optical scenes, the proposed model demonstrated robust performance comparable to or exceeding previous multi-sensor studies. These results underscore the potential of combining freely available Landsat 9 time-series data with attention-enhanced deep learning methods for efficient and scalable crop classification. The findings emphasize the important role of NIR reflectance during key growth stages and the effectiveness of TCN architectures in modeling temporal spectral variations for agricultural monitoring applications.

1. Introduction

With the rapid growth of the global population and the increasing demand for agricultural productivity, accurate land cover and crop classification, as well as the identification of the spatial distribution of various crops, have become crucial for governments, policymakers, and farmers to improve agricultural decision-making (Gómez et al., 2016). The production of thematic maps—such as land use/land cover (LULC) and crop type maps—from remote sensing data represents one of the most important applications of remote sensing, because it provides periodic and scalable information for monitoring agricultural activities (Roy et al., 2014).

Remote sensing has gained considerable attention in agriculture due to its ability to provide regional and temporal information for crop monitoring and thematic mapping (Kim et al., 2017; Kwak and Park, 2019). Numerous studies have focused on generating reliable thematic maps from remote sensing data (Tsuchiya, et al., 2025). From a data availability perspective, multi-source datasets—including optical, synthetic aperture radar (SAR), and geographic information system data—have been used for classification tasks (Kim et al., 2017). Among these, the Landsat satellite series has been one of the most important sources of data for studying land cover changes such as deforestation, agricultural expansion, urbanization, and wetland loss (Zhu and Woodcock, 2014). The release of the Landsat archive as free and open data in 2008 greatly increased its use by removing access barriers and broadening research applications (Woodcock et al., 2008; Wulder et al., 2008). Thanks to the "time machine" capability of the Landsat archive, it is now widely used for long-term land cover and land use change assessments (Hansen and Loveland, 2012; Potapov et al., 2020; Wulder et al., 2016). Therefore, this study explores the potential of Landsat 9 data for crop classification.

Machine learning techniques have become increasingly important in agriculture, especially for enhancing crop productivity and quality (Tariq et al., 2023). Among common supervised learning methods, random forest (RF) is advantageous in handling high-dimensional data and remains robust when data are incomplete or insufficient (Luo et al., 2023). Similarly, support vector machines (SVMs) are widely applied in remote sensing for LULC mapping and crop classification due to their strong theoretical foundation in statistical learning (Moumni and Lahrouni, 2021; Wang et al., 2019). However, both RF and SVM have limitations in modeling temporal dependencies, because they are not designed to work directly with time-series data (Ndikumana et al., 2018).

Temporal features are vital for crop classification because crops exhibit unique spectral and structural patterns across different phenological stages (Qu et al., 2020). Deep learning has emerged as a powerful tool for extracting discriminative temporal features from dense optical time-series data, even when observations are missing (Zhao et al., 2021). Among deep learning approaches, recurrent neural networks (RNNs) are particularly suited for sequential data analysis (Filho et al., 2020; Mou, et al., 2018). However, RNNs can suffer from vanishing or exploding gradient problems when modeling long-term dependencies (Duan et al., 2023). To overcome this issue, variants such as long short-term memory (LSTM) networks and bidirectional gated recurrent units (Bi-GRUs) have been developed (Deng et al., 2018). LSTM networks demonstrate superior ability to capture long-term temporal dependencies, supporting large-scale crop type mapping (Feng et al., 2023). Likewise, Bi-GRU networks efficiently capture contextual information by processing data in both forward and backward directions (Duan et al., 2023; Kim and Lee, 2017).

Temporal convolutional networks (TCNs) have also emerged as a competitive alternative to RNNs. They use causal and dilated convolutions, ensuring the output at time t depends only on previous inputs, thereby preserving temporal causality (Liu et al., 2024). Research has shown that TCNs can outperform traditional RNNs in various sequence modeling tasks (Bai et al., 2018).

In this study, we conducted crop classification using three RNN-based methods—LSTM, Bi-GRU, and TCN—on Landsat 9 data and evaluated their comparative performance. Additionally, we incorporated an attention mechanism that mimics human visual perception by focusing computational resources on the most informative regions of the input data (Larochelle and Hinton,

This contribution has been peer-reviewed. The double-blind peer-review was conducted on the basis of the full paper.
https://doi.org/10.5194/isprs-annals-XI-3-2026-821-2026

2010; Mnih et al., 2014; Xu et al., 2018). Previous studies have shown that combining attention mechanisms with RNNs improves crop classification accuracy (Tsuchiya and Sonobe, 2025). Therefore, we applied attention-based models to further enhance classification performance in this study.

2. Materials and Methods

2.1 Study Area

This study was conducted in the Tokachi Plain, located in southeastern Hokkaido, Japan, between 142°48′13″ and 143°8′52″ E longitude and 42°43′47″ and 43°7′29″ N latitude (Figure 1). The region has a continental humid climate with warm summers and cold, snowy winters, an average annual temperature of approximately 6°C, and annual precipitation of about 920 mm. The fertile volcanic ash soil and well-developed irrigation systems make the Tokachi Plain one of Japan’s leading agricultural production regions.

The area benefits from extended daylight hours during the growing season, allowing the cultivation of a wide range of crops. This study focused on the major crops typical of mixed farming in the Tokachi Plain, including soybeans, adzuki beans, kidney beans, maize, beetroot, potatoes, and forage grasses. Beans and maize are typically sown in mid-May, while beetroot and potatoes are planted between late April and early May. Perennial grasses and winter crops such as timothy, orchardgrass, and winter wheat are sown in the previous year. Harvest times differ by crop: beans are harvested from late September to early November, beetroot in November, potatoes from late August through September, and winter wheat from late July to early August. Forage grasses are harvested twice per year—once from late June to early July and again in late August—playing a vital role in supporting the region’s dairy and livestock industries.

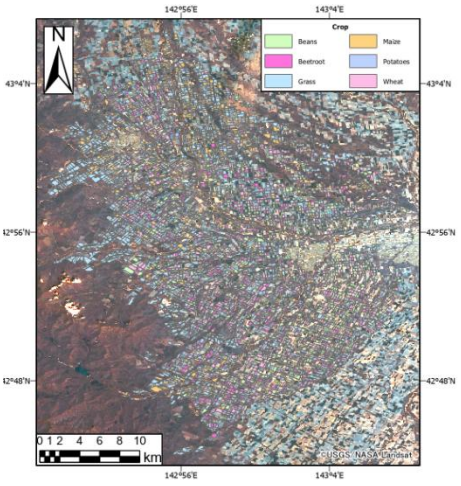

Figure 1. Location of the study area in Hokkaido, Japan. The enlarged map shows Landsat 9 imagery acquired on June 28, 2024 (downloaded from EarthExplorer/United States Geological Survey, USGS), providing spatial details of the region. The crop map was generated from geographic information system vector data obtained from the Ministry of Agriculture, Forestry, and Fisheries (MAFF)’s open data portal.

2.2 Reference Data

Farmland boundary data were obtained from the Ministry of Agriculture, Forestry, and Fisheries (MAFF) open data portal (https://open.fude.maff.go.jp/) and used as reference information for this study. A total of 8,308 agricultural fields were analyzed using Landsat imagery, including 1,435 bean fields, 726 beetroot fields, 2,287 grasslands, 1,113 maize fields, 902 potato fields, and 1,845 winter wheat fields. The total area (in hectares) for each crop type is summarized in Table 1. The reference data represent crops cultivated between June and August 2024, and no crop rotation or land cover changes occurred during the Landsat 9 data acquisition period.

Table 1. Summary of agricultural fields analyzed in this study

	Number Fields	Area(ha)				
		Minimum	Median	Mean	Maximum	Standard Deviation
Beans	1,435	0.07	2.46	3.09	31.05	2.07
Beetroot	726	0.06	2.53	3.05	14.36	1.77
Grass	2,287	0.06	2.23	2.98	33.38	3.04
Maize	1,113	0.05	2.45	2.92	31.22	2.34
Potatoes	902	0.25	2.48	2.95	15.00	1.75
Wheat	1,845	0.10	2.64	2.89	19.78	2.00

2.3 Satellite Data

Since its launch in the 1970s, NASA’s Landsat program has become one of the most widely used satellite data sources for Earth surface mapping (Gómez et al., 2016; Masek et al., 2020; Roy et al., 2014). For this study, we used the latest dataset, Landsat 9, which was downloaded from the United States Geological Survey EarthExplorer platform (https://earthexplorer.usgs.gov/).

Landsat 9 operates in a near-polar orbit at approximately 705 km altitude, with a 16-day revisit cycle and a 185 km swath width. It is equipped with two sensors: the Operational Land Imager-2 (OLI-2) and the Thermal Infrared Sensor-2 (TIRS-2) (Table 2). OLI-2 includes the Coastal/Aerosol (Ultra Blue), Blue, Green, Red, Near-Infrared (NIR), Shortwave Infrared 1 (SWIR1), Shortwave Infrared 2 (SWIR2), Panchromatic, and Cirrus bands. The Cirrus band is mainly used for cloud detection and atmospheric correction, while TIRS-2 measures land surface temperature.

For crop classification, we used the Coastal/Aerosol (Ultra Blue), Blue, Green, Red, NIR, SWIR1, and SWIR2 bands. Six cloud-free Landsat 9 scenes (OLI-2), acquired between May 2 and September 16, 2024, were analyzed in this study (summarized in Table 3).

Table 2. Spectral characteristics of Landsat 9 Operational Land Imager-2 (OLI-2)/Thermal Infrared Sensor-2 (TIRS-2) sensors (source: USGS)

Satellite	Sensor	Band (Wavelength / μm)	Spectral region	Spatial resolution (m)
Landsat 9	OLI-2 / TIRS-2	1 (0.43 - 0.45)	Ultra blue (coastal/aerosol)	30
		2 (0.45 - 0.51)	Blue	30
		3 (0.53 - 0.59)	Green	30
		4 (0.64 - 0.67)	Red	30
		5 (0.85 - 0.88)	NIR	30
		6 (1.57 - 1.65)	SWIR1	30
		7 (2.11 - 2.29)	SWIR2	30
		8 (0.50 - 0.68)	Panchromatic	15
		9 (1.36 - 1.38)	Cirrus	30
		10 (10.60 - 11.19)	Thermal Infrared (TIR1)	100
		11 (11.50 - 12.51)	Thermal Infrared (TIR2)	100

Table 3. Details of satellite data used in this study

Acquisition DateTime	Scene ID	Instruments	Sun Azimuth	Sun Elevation
2024/5/2	LC91070302024123LGN00	OLI-2	144.6	58.1
2024/5/18	LC91070302024139LGN00	OLI-2	140.9	61.8
2024/6/12	LC91060302024164LGN00	OLI-2	135.2	64.4
2024/6/28	LC91060302024180LGN00	OLI-2	133.6	64.0
2024/7/5	LC91070302024187LGN00	OLI-2	133.7	65.4
2024/9/16	LC91060302024260LGN00	OLI-2	153.6	46.3

2.4 Classification Model Structure

Temporal prediction tasks require dynamic classifiers that can model sequential dependencies. Unlike feedforward neural networks, RNNs incorporate feedback connections, allowing the model to utilize information from previous time steps (Werbos, 1990; Williams and Zipser, 1989). However, standard RNNs suffer from vanishing or exploding gradients when modeling long-term dependencies, typically beyond about ten time steps.

The LSTM network overcomes this limitation by introducing a memory cell structure with three gates (input, forget, and output) that regulate information flow (Suebsombut et al., 2021; Yu et al., 2019). The input gate controls when new information enters the cell, the forget gate decides which past information to retain, and the output gate determines how stored information is used for prediction.

The Bi-GRU network enhances the traditional GRU by processing data in both forward and backward directions, thus capturing dependencies from past and future contexts (Amiri et al., 2024; Mao et al., 2021; Tsuchiya and Sonobe, 2025; Wang et al., 2022; Xu et al., 2022). Compared to LSTM, GRU models are more computationally efficient while maintaining comparable performance. This bidirectional design is particularly advantageous for time-series classification tasks such as crop type mapping, where both previous and subsequent spectral patterns can improve discrimination accuracy.

TCNs represent another approach for sequence modeling, consisting of stacked one-dimensional convolutional layers with causal and dilated convolutions. The causality constraint ensures that each time step depends only on the current and previous inputs, thereby preserving temporal order (Yli-Heikkilä et al., 2025). Following previous research (Luo, et al., 2023; Pelletier, et al., 2019; Tsuchiya, et al., 2025), we used 64 filters per convolutional layer, a kernel size of 3, residual connections, rectified linear unit activation, and dropout regularization. Because TCNs process data in parallel rather than sequentially, they achieve faster training and better scalability for large time-series datasets such as multi-temporal satellite imagery.

Because LSTM, Bi-GRU, and TCN models can effectively capture temporal dependencies and learn noise-resistant patterns directly from raw data, no time-series interpolation or smoothing was applied. Model performance was evaluated through cross-validation, with hyperparameters tuned to minimize loss. Early stopping and regularization were implemented to prevent overfitting.

2.5 Classification Process

Figure 2 outlines the overall classification workflow. To emphasize spectral reflectance differences among crop types, polygon data were used instead of raster data. To reduce mixed-pixel effects (caused by spectral blending near field boundaries), a 10-m inward buffer was applied to each field polygon. The buffered polygons were then used to extract mean reflectance values from Bands 1–7 for each field across all six Landsat 9 scenes.

To address class imbalance among crop types, we applied the synthetic minority oversampling technique (SMOTE). For each minority-class sample, nearest neighbors were identified, and synthetic samples were generated along line segments connecting the sample to its neighbors (Mukherjee and Khushi, 2021). Specifically, we used k-means SMOTE, which restricts synthetic sample generation to “safe” cluster regions, reducing the influence of noisy data (Zhu et al., 2023).

A 10-fold cross-validation procedure was used for classification, maintaining equal proportions of all six classes within each fold. Ninety percent of the data were used for training, and 10% for testing. Within the training set, 20% were reserved for validation and hyperparameter tuning.

All preprocessing and model training were performed using Google Colab. Classification performance was measured using overall accuracy (OA), kappa coefficient, producer’s accuracy (PA), user’s accuracy (UA), and F1 score. McNemar’s test was used to determine whether differences in performance between models were statistically significant.

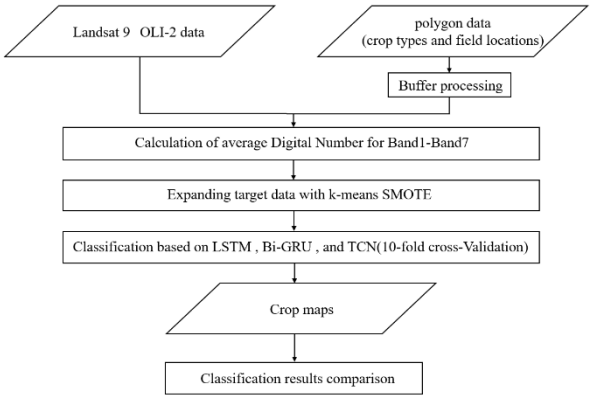

Figure 2. Workflow overview of the crop classification process.

3. Results

3.1 Temporal Changes in Digital Numbers

The classification results for each model are shown in Figure 3. The temporal patterns of DNs obtained from Landsat 9 OLI-2 effectively represent the crops’ phenological stages throughout the growing season.

On May 2, most fields had not yet been sown or transplanted, so the DNs mainly represented surface conditions such as residual vegetation from the previous growing season and high soil moisture caused by snowmelt. As a result, inter-crop differences in DNs were minimal across all spectral bands during this period. As the growing season advanced toward July, DNs diverged noticeably among crop types, corresponding to differences in canopy development and biomass accumulation. Notably, Band 5 (NIR) showed the greatest variation among crop species, consistent with its high sensitivity to vegetation structure and chlorophyll content.

3.2 Crop Classification Accuracies

The classification results from 10-fold cross-validation and McNemar’s test are summarized in Tables 4 and 5 respectively. Among the evaluated models—LSTM + Attention, Bi-GRU + Attention, and TCN + Attention—the TCN + Attention model achieved the highest OA of 81.3%.

Statistical comparisons using McNemar’s test revealed significant differences ($p < 0.001$) between all model pairs:

- LSTM + Attention vs. Bi-GRU + Attention
- LSTM + Attention vs. TCN + Attention
- Bi-GRU + Attention vs. TCN + Attention

This indicates that the TCN + Attention architecture provided significantly better classification performance than the other two models.

This contribution has been peer-reviewed. The double-blind peer-review was conducted on the basis of the full paper.
https://doi.org/10.5194/isprs-annals-XI-3-2026-821-2026 | © Author(s) 2026. CC BY 4.0 License.

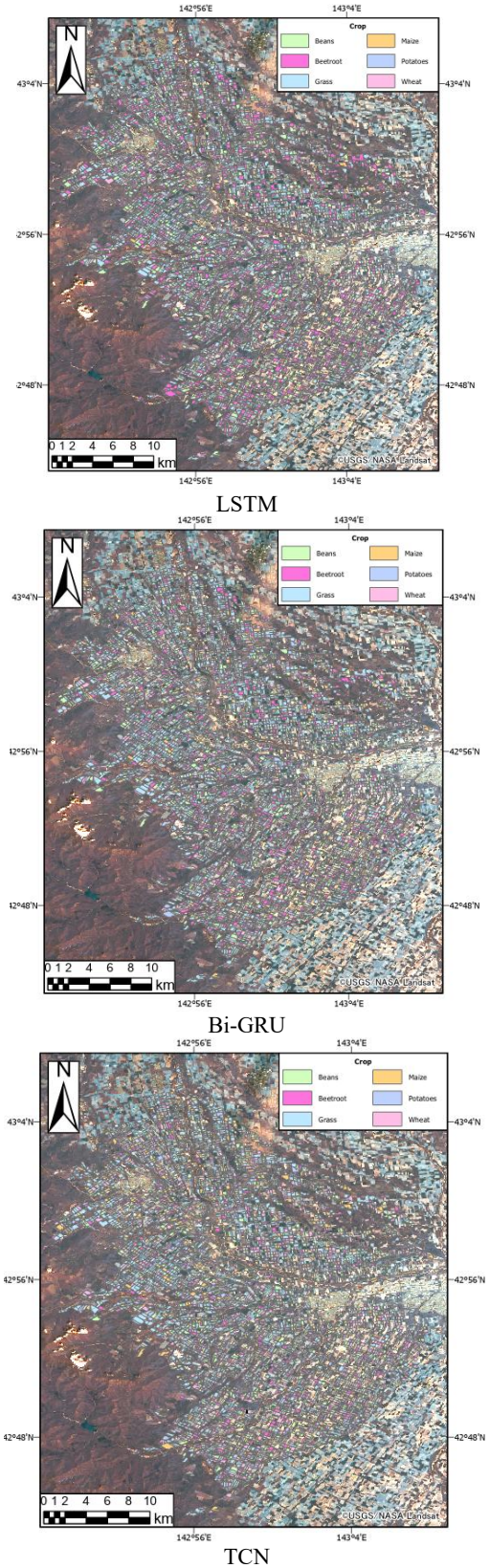

Figure 3. Crop classification maps generated by LSTM + Attention, Bi-GRU + Attention, and TCN + Attention models.

Table 4. Classification accuracies obtained using 10-fold cross-validation. Underlined values show the highest score for each class and metric

	Crop	LSTM+Attention	Bi-GRU+Attention	TCN+Attention
PA				
	Beans	66.1%	78.7%	81.3%
	Beetroot	78.0%	83.0%	75.6%
	Grass	64.9%	82.0%	88.3%
	Maize	4.6%	13.7%	62.0%
	Potatoes	12.0%	32.3%	63.1%
	Wheat	28.8%	55.8%	95.4%
UA				
	Beans	39.4%	60.0%	73.7%
	Beetroot	26.9%	45.1%	80.0%
	Grass	66.4%	74.1%	95.7%
	Maize	17.9%	34.6%	72.9%
	Potatoes	16.7%	44.5%	75.5%
	Wheat	44.1%	74.6%	87.5%
F1				
	Beans	47.8%	67.4%	76.0%
	Beetroot	38.2%	57.0%	76.4%
	Grass	60.1%	76.8%	91.8%
	Maize	7.3%	16.4%	62.4%
	Potatoes	13.2%	32.8%	67.8%
	Wheat	31.8%	61.3%	91.1%
	OA	44.4%	61.2%	81.3%
	Kappa	0.332	0.520	0.769

Table 5. Results of McNemar’s test. *** indicates statistical significance at the 0.1% level

	LSTM + Attention	Bi-GRU + Attention	TCN + Attention
LSTM + Attention		***	***
Bi-GRU + Attention			***
TCN + Attention			

3.3 Importance of Each Variable

The relative importance (attention weights) of Bands 1–7 across six observation dates was visualized as heatmaps to identify which spectral and temporal features contributed most to classification accuracy (Figure 4).

Across all models, Bands 5–7—especially Band 5 (NIR)—consistently showed the highest importance values, highlighting their significant role in distinguishing vegetation types. For the Bi-GRU + Attention and TCN + Attention models, data from May 18 (T2) onward—corresponding to early-to-mid growing stages—showed relatively higher importance. This suggests that discriminative spectral characteristics emerge after initial crop establishment, as canopy structure and leaf area begin to diverge among crop types.

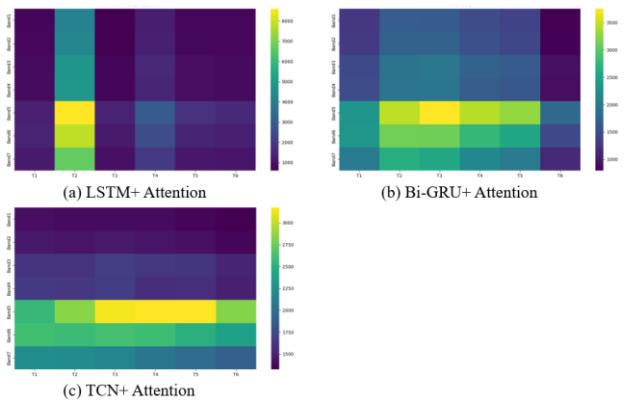

Figure 4. Temporal changes in the importance of each spectral band across six observation dates.

4. Discussion

Several previous studies have combined optical, SAR, and radar data for crop type classification, typically achieving OAs around 80%, depending on crop type, study area, and modeling approach. For instance, Ferrant et al. (2017) used an RF classifier with Sentinel-1 and Sentinel-2 data to map major crops, reporting an OA exceeding 80%. Similarly, Schultz et al. (2015) applied image segmentation and RF algorithms to classify crops in Brazil using Landsat 8 and RapidEye data, achieving approximately 80% accuracy.

In this study, we applied an attention-based TCN to classify six major crops in the Tokachi Plain, Hokkaido, achieving an OA of 81.3%. Despite challenges in distinguishing crops with similar phenological patterns—such as beans and maize—and using only Landsat 9 optical data, our classification accuracy matches or exceeds that of previous multi-sensor studies.

This strong performance can be attributed to three main factors:
(1) the rich spectral information provided by Landsat 9’s seven bands;
(2) the relatively large amount of available training data; and
(3) the use of an advanced deep learning architecture capable of effectively capturing temporal dynamics.

These results highlight the potential of combining freely available optical satellite time-series data with state-of-the-art deep learning techniques—particularly those incorporating attention mechanisms—to improve crop classification accuracy.

Analysis of attention weights showed that Band 5 (NIR) was consistently the most influential feature across all models. Vegetation indices such as the enhanced vegetation index and normalized difference vegetation index, which rely on NIR reflectance, have been widely used in previous studies (Wardlow et al., 2007) and effectively capture seasonal vegetation dynamics. Although vegetation indices were not explicitly used here, the importance of the NIR band suggests similar patterns, confirming its strong association with crop phenology.

For the TCN + Attention model, the importance of the NIR band increased notably from June to July, corresponding to the rapid growth phase of most crops. This suggests that the NIR band effectively captured differences in crop biophysical characteristics during key developmental stages, substantially enhancing classification performance.

Among the three deep learning architectures evaluated, TCN consistently outperformed LSTM and Bi-GRU. This aligns with previous work (Tsuchiya and Sonobe, 2025) and is attributed to TCNs’ hierarchical dilated convolutional structure, which better captures long-term temporal dependencies. The use of dilated and causal convolutions allows TCNs to retain historical information efficiently while maintaining high computational speed (Zhang et al., 2025). Because optical time-series data inherently reflect seasonal variations in crop growth, the TCN structure provides a more efficient and accurate way to model these temporal patterns than recurrent models.

Because optical satellite imagery is often affected by cloud cover, classification accuracy can vary depending on acquisition timing and image availability. Nevertheless, despite relying on only six cloud-free images in this study—and none from August, when morphological differences among crops are usually most pronounced—the TCN + Attention model still achieved an OA exceeding 80%. This demonstrates the robustness of the method and its potential for operational crop classification using freely available optical satellite data.

According to Yin et al (Yin, et al., 2025)., the average annual probability of obtaining observation data over Asia from Landsat 8, which has the same revisit period as Landsat 9, is 42.46% with a cloud coverage rate of 24% or less. During the period from May to September covered by this study, there were approximately 10 possible acquisitions, and only six images were actually used, resulting in an image acquisition rate that exceeds the average for Asia. However, this study only used Landsat 9, and using Landsat 8 in combination increases the opportunities for data acquisition, so it is expected to be used in other regions as well. Even so, caution is required when targeting regions such as Europe, where the probability of obtaining Landsat data is lower than in other regions (Yin, et al., 2025).

In this study, a classification accuracy of over 80% was achieved even under conditions including small fields of approximately 100 m². This result demonstrates the practical feasibility of crop classification using satellite images for small plots of land. Furthermore, in recent years, several optical satellites with higher spatial resolution than Landsat 9 have become available, and using these data may further improve classification accuracy.

In terms of class-specific accuracies, grass exhibited the highest PA, UA, and F1 scores, likely due to its abundance in the study area and the model’s ability to effectively learn its distinct spectral-temporal features. Conversely, maize had the lowest PA, UA, and F1 scores. This is likely due to the relatively small number of maize fields and the spectral similarity of maize and potato time-series profiles, especially before mid-June, which probably led to higher misclassification rates.

Although the k-means SMOTE method was applied to mitigate class imbalance, the models still performed best for grass and wheat, which had the largest sample sizes. To develop a more generalizable crop classification framework, it will be important to improve performance for minority crop classes. Future research should therefore focus on advanced data augmentation or sampling techniques to enhance model robustness under class imbalance. Furthermore, when applying this approach to different regions and years, using existing models as is may result in a decrease in accuracy, so it is desirable to retrain using training data collected in the target region. In this study's method, classified samples obtained through field survey data, administrative documents, and labeling using high-resolution images are essential for parameter learning. However, additional verification across multiple time periods and multiple regions is required to determine whether this study's approach can actually be generalized.

Overall, the findings of this study underscore the effectiveness of Landsat 9’s seven-band time-series data for discriminating multiple crop species. With its global coverage, consistent revisit cycle, and rich spectral information, Landsat 9 remains a cornerstone platform for optical satellite-based agricultural monitoring. Moving forward, it will be essential to validate and harness data from both current and future Landsat missions to further enhance temporal crop classification capabilities. The temporal spectral dynamics captured by Landsat 9 offer valuable biophysical insights into crop growth, harvesting, and senescence, reinforcing its important role in supporting sustainable agricultural management.

5. Conclusions

In this study, we evaluated the classification performance of six major crops in the Tokachi Plain, Hokkaido, using time-series Landsat 9 data (Bands 1–7) acquired between May 2 and September 16, 2024. Three deep learning architectures—LSTM, Bi-GRU, and TCN—each incorporating an attention mechanism, were assessed for crop type classification. Among these, the TCN with attention achieved the highest OA of 81.3%, demonstrating superior capability in modeling temporal dependencies in multispectral satellite data.

The analysis of attention weights showed that imagery acquired after May 18, marking the onset of active crop growth, provided the most discriminative spectral information in both the Bi-GRU

+ Attention and TCN + Attention models. In contrast, data from May 2 contributed less to classification accuracy due to minimal vegetative development at that time.
Overall, the results demonstrate that integrating TCNs with attention mechanisms significantly improves crop classification accuracy using freely available Landsat time-series data. This approach has strong potential for operational agricultural monitoring and large-scale crop mapping in regions with similar climatic and cropping conditions.

Acknowledgments

This work was supported by JSPS KAKENHI Grant Number 25K09353.

References

Amir, A. F., Kichou, S., Oudira, H., Chouder , A., & Silvestre, S. (2024). Fault Detection and Diagnosis of a Photovoltaic System Based on Deep Learning Using the Combination of a Convolutional Neural Network (CNN) and Bidirectional Gated Recurrent Unit (Bi-GRU). Sustainability, 16(3), 1012. doi:doi.org/10.3390/su16031012

B., L. T., B., C. U., M., A. R., & A., J. J. (2023). Temporal Convolutional Neural Network for Land Use and Land Cover. Arab. J. Geosci, 16, 585. doi:DOI:10.1007/s12517-023-11688-4
Bai, S., Kolter, J. Z., & Koltun, V. (2018). An Empirical Evaluation of Generic Convolutional and Recurrent Networks for Sequence Modeling. arXiv, 1803.01271. doi:doi.org/10.48550/arXiv.1803.01271

D.P. Roy, M. W., Roy, D. P., Wulde, M. A., Loveland, T. R., & Woodcock, C. E. (2014). Landsat-8: Science and product vision for terrestrial global change research. Remote Sensing of Environment, 145-172. doi:doi.org/10.1016/j.rse.2014.02.001

Deng, T., He, X., & Zeng, Z. (2018). Recurrent neural network for combined economic and emission dispatch. Appl. Intell, 48, 2180–2198. doi:DOI:10.1007/s10489-017-1072-3

Duan, Y., Liu, Y., Wang, Y., & Ren, S. (2023). Improved BIGRU Model and Its Application in Stock Price Forecasting. electronics, 12(12), 2718. doi:doi.org/10.3390/electronics12122718

Feng, F., Gao, M., Liu, R., & Yao, S. (2023). A deep learning framework for crop mapping with reconstructed Sentinel-2 time series images. Computers and Electronics in Agriculture, Volume 213,108227. doi:doi.org/10.1016/j.compag.2023.108227

Fengmin SunLianShujun. (2022). ν -Improved nonparallel support vector machine. Scientific Reports, 12(1). doi:doi.org/10.1038/s41598-022-22559-5
Ferrant, S., Selles, A., Page, M. L., Herrault, P. A., Pelletier, C., Bitar, A. A., . . . Kerr, Y. (2017). Detection of Irrigated Crops from Sentinel-1 and Sentinel-2 Data to Estimate Seasonal Groundwater Use in South India. Remote Sensing, 9(11), 1119. doi:doi.org/10.3390/rs9111119

Fukang FengGao,Ronghua Liu,shuihong Yao,Guijun YangMaofang. (2023). A deep learning framework for crop mapping with reconstructed Sentinel-2 time series images. Computers and Electronics in Agriculture, Volume 213, 108227. doi:doi.org/10.1016/j.compag.2023.108227

GómezCristina, White C. Joanne , WulderA.Michael. (2016). Optical remotely sensed time series data for land cover classification: A review. ISPRS Journal of Photogrammetry and Remote Sensing, 55-72. doi:doi.org/10.1016/j.isprsjprs.2016.03.008

Hansen, M., & Loveland, T. (2012). A review of large area monitoring of land cover change using Landsat data. Remote. Sens. Environ., 122, 66–74. doi:doi.org/10.1016/j.rse.2011.08.024

Kim J., LeeJ. (2017). Multiple Range-Restricted Bidirectional Gated Recurrent Units with Attention for Relation Classification. arXiv, 1707.01265. doi:doi.org/10.48550/arXiv.1707.01265

Kim Yeseul , Park No-Wook and Lee andKyung-Do (2017). Self-Learning Based Land-Cover Classification Using Sequential Class Patterns from Past Land-Cover Maps. remote sensing, 9(9), 921. doi:doi.org/10.3390/rs9090921

KwakORC, G.-H., & Park, N.-W. (2019). Impact of Texture Information on Crop Classification with Machine Learning and UAV Images. applied sciences, 9(4), 643. doi:doi.org/10.3390/app9040643

Lahrouni, Moumni, A., & Abderrahman. (2021). Machine Learning-Based Classification for Crop-Type Mapping Using the Fusion of High-Resolution Satellite Imagery in a Semiarid Area. Scientifica, 20. doi:doi/10.1155/2021/8810279?msockid=31acd2f28f4c695f3018c6ae8ed5685b

LarochelleH., HintonG.E. (2010). Learning to combine foveal glimpses with a third-order boltzmann machine. In Proceedings of the Advances in Neural Information Processing Systems (NIPS). Vancouver, BC, Canada, 1243−1251. doi:dl.acm.org/doi/10.5555/2997189.2997328

Liu Shujun, Xu Tong, Du Xiaoze, Zhang Yaocong, Wu Jiangbo (2024). A hybrid deep learning model based on parallel architecture TCN-LSTM with Savitzky-Golay filter for wind power prediction. Energy Conversion and Management, Volume 30,118122. doi:doi.org/10.1016/j.enconman.2024.118122

Luo, K., Lu, L., Xie, Y., Chen, F., & yin, F. (2023). Crop type mapping in the central part of the North China Plain using Sentinel-2 time series and machine learning. Computers and Electronics in Agriculture, Volume 205,107577.doi:doi.org/10.1016/j.compag.2022.107577

Mao, X., Zhang, F., Wang, G., Chu, Y., & Yua, K. (2021). Semi-random subspace with Bi-GRU: Fusing statistical and deep representation features for bearing fault diagnosis. Measurement, Volume 173,108603. doi:doi.org/10.1016/j.measurement.2020.108603

Masek,, J. G., Wulder, M. A., & Markham, B. (2020). Landsat 9: Empowering open science and applications through continuity. Remote Sensing of Environment, 111968. doi:doi.org/10.1016/j.rse.2020.111968

MnihV., HeessN., GravesA. (2014). Recurrent models of visual attention. In Proceedings of the Advances in Neural Information Processing Systems (NIPS). Montreal, QC, Canada, 2204−2212.

https://proceedings.neurips.cc/paper_files/paper/2014/file/3e456b31302cf8210edd4029292a40ad-Paper.pdf

Mohammad-ParsaH., LuS., KamarajK., SlowikowskiA., HaygreevC.V. (2019). Deep learning architectures. In Deep learning: Concepts and Architectures; Springer: Berlin/Heidelberg, 1−24. doi:DOI:10.1007/978-3-030-31756-0_1

MouLichao, BruzzoneLorenzo, ZhuXiangXiao. (2018). Learning Spectral-Spatial-Temporal Features via a Recurrent Convolutional Neural Network for Change Detection in Multispectral Imagery. IEEE Transactions on Geoscience and Remote Sensing, Volume: 57, Issue: 2,924 - 935. doi:DOI: 10.1109/TGRS.2018.2863224

Mukherjee, M., & Khushi, M. (2021). SMOTE-ENC: A Novel SMOTE-Based Method to Generate Synthetic Data for Nominal and Continuous Features. Appl. Syst. Innov, 4(1), 18. doi:doi.org/10.3390/asi4010018

Ndikumana, E., Ho, D., Minh, T., & Baghdad, N. (2018). Deep Recurrent Neural Network for Agricultural Classification using multitemporal SAR Sentinel-1 for Camargue, France. remote sensing, 10(8), 1217. doi:doi.org/10.3390/rs10081217

Potapov, P., Hansen, M. C., & Komm, I. (2020). Landsat Analysis Ready Data for Global Land Cover and Land Cover Change Mapping. remote sens., 12(3), 426. doi:doi.org/10.3390/rs12030426

Qu, Y., Zhao, W., Yuan , Z., & Chen, J. (2020). Crop Mapping from Sentinel-1 Polarimetric Time-Series with a Deep Neural Network. remote sensing, 12(15), 2493. doi:doi.org/10.3390/rs12152493

Schultz, B., Immitzer, M., Formaggio, A. R., Sanches, I. D., Luiz, A. J., & Atzberger, C. (2015). Self-Guided Segmentation and Classification of Multi-Temporal Landsat 8 Images for Crop type Mapping in Southeastern Brazil. Remote Sensing., 7(11), 14482-14508. doi:doi.org/10.3390/rs71114482

Suebsombut, P., Sekhari, A., & Sureeph, P. (2021). Field Data Forecasting Using LSTM and Bi-LSTM Approaches. Applied Sciences, 11(24), 11820. doi:doi.org/10.3390/app112411820

Tao HeSun, Ji-De Xu, Xue-Jun Wang, Chang-Ru HuYu-Jun. (2014). Enhanced land use/cover classification using support vector machines and fuzzy k-means clustering algorithms. Journal of Applied Remote Sensing, 8(1). doi:doi.org/10.1117/1.jrs.8.083636

Tariq, A., Yan, J., Gagnon, A. S., Khan, M. R., & Mumtaz, F. (2023). Mapping of cropland, cropping patterns and crop types by combining optical remote sensing images with decision tree classifier and random forest. Geo-spatial Information Science, Volume 26,Pages 302-320. doi:DOI:10.1080/10095020.2022.2100287

Tsuchiya, Y., & Sonobe, R. (2025). Crop Classification Using Time-Series Sentinel-1 SAR Data:. remote sensing, 17(12), 2095. doi:doi.org/10.3390/rs17122095

Wang, L., Dong, Q., Yang, L., & Gao , J. (2019). Crop Classification Based on a Novel Feature Filtering and Enhancement Method. remote sensing, 11(4), 455. doi:DOI:10.3390/rs11040455

Wang, Y., Zheng, D., & Jia, R. (2022). Fault Diagnosis Method for MMC-HVDC Based on Bi-GRU Neural Network. Energies, 15(3), 994. doi:doi.org/10.3390/en15030994

Wardlow, B. D., Egbert , S. L., & Kastens, J. H. (2007). Analysis of time-series MODIS 250 m vegetation index data for crop classification in the U.S. Central Great Plains. Remote Sensing of Environment, Volume 108, Issue 3,,290-310. doi:doi.org/10.1016/j.rse.2006.11.021

Werbos, P. J. (1990). Backpropagation through time: what it does and how to do it. Proceedings of the IEEE, 1550 - 1560. doi:DOI: 10.1109/5.58337

Williams, R. J., & Zipser, D. (1989). A Learning Algorithm for Continually Running Fully Recurrent Neural Networks. Neural Computation, 270 - 280. doi:DOI: 10.1162/neco.1989.1.2.270

Woodcock, C., Allen, R., Anderson, M., Belward, A., Bindschadler, R., Cohen, W., . . . al., e. (2008). Free Access to Landsat Imagery. Science, 320, 1011. doi:DOI:10.1126/science.320.5879.1011a

Wulder, M., White, J., Goward, S., Masek, J., Irons, J., Herold, M., . . . Woodcock, C. (2008). Landsat continuity: Issues and opportunities for land cover monitoring. Remote. Sens. Environ, 112, 955–969. doi:doi.org/10.1016/j.rse.2007.07.004

Xu, H., Zhang, A., Xu, X., Li, P., & Ji, Y. (2022). Prediction of Particulate Concentration Based on Correlation Analysis and a Bi-GRU Model. International Journal of Environmental Research and Public Health, 19(20), 13266. doi:doi.org/10.3390/ijerph192013266

Xu, R., Tao, Y., Lu, Z., & Zhon, y. (2018). Attention-Mechanism-Containing Neural Networks for High-Resolution Remote Sensing Image Classification. remote sensing, 10(10), 1602. doi:doi.org/10.3390/rs10101602

Yin, Y., Peng, L., Zhiming , F., Suresh, R. C., & Hong, Y. (2025). Global Landsat image acquisition probability: 1984–2023. International Journal of Applied Earth, Volume 144, 104928. doi:doi.org/10.1016/j.jag.2025.104928

Yli-HeikkiläMaria , KlamiArto , WittkeSamantha , LuotamoMarkku , MeroPinja , PellikkaPetri. (2024). Tillage and biomass detection for estimating winter-time cropland management practices with satellite remote sensing. European Journal of Remote Sensing, Volume 58, 2025. doi:doi.org/10.1080/22797254.2025.2525967

Yu, Y., Si, X., Hu, C., & Zhang, J. (2019). A review of recurrent neural networks: LSTM cells and network architectures. Neural Comput, 31, 1235–1270. doi:DOI:10.1162/neco_a_01199

Zhang, L., Ren , G., Li, S., Du, J., Xu, D., & Li , Y. (2025). A novel soft sensor approach for industrial quality prediction based TCN with spatial and temporal attention. Chemometrics and Intelligent Laboratory, Volume 257, 15,105272. doi:doi.org/10.1016/j.chemolab.2024.105272

Zhao, H., Duan, S., Liu, J., & Sun, L. (2021). Evaluation of Five Deep Learning Models for Crop Type Mapping Using

Sentinel-2 Time Series Images with Missing Information. remote sensing, 13(14), 2790. doi:doi.org/10.3390/rs13142790

Zhu, X., Zhang, H., Ren, Q., Zhang, D., Zeng, F., Zhu, X., & Zhang, L. (2023). An automatic identification method of imbalanced lithology based on Deep Forest and K-means SMOTE. Geoenergy Science and Engineering, Volume 224, 211595. doi:doi.org/10.1016/j.geoen.2023.211595

Zhu, Z., & Woodcock, C. E. (2014). Continuous change detection and classification of land cover using all available Landsat data. Remote Sensing of Environment, 152-171. doi:doi.org/10.1016/j.rse.2014.01.011